OPEN

Switching suppression and enhancement of fluorescence and six-wave mixing by phase modulation

Zhiguo Wang, Peng Ying, Peiying Li, Dan Zhang, Heqing Huang, Hao Tian & Yanpeng Zhang

Key Laboratory for Physical Electronics and Devices of the Ministry of Education & Shaanxi Key Lab of Information Photonic Technique, Xi'an Jiaotong University, Xi'an 710049, China.

The conversion between enhancement and suppression in six-wave mixing (SWM) and fluorescence signals by phase modulation has demonstrated for the first time. It is observed in our experiment the suppression of SWM and fluorescence is transformed into enhancement in company with the switch from electromagnetically induced transparency (EIT) to electromagnetically induced absorption (EIA) in the transmitted probe with the relative phase changed from 0 to $\pi/2$. Our research could be potentially applied in optical communication and quantum information processing.

Lots of studies focus on the electromagnetically induced transparency (EIT) and the higher-order nonlinear optical process comprising four-wave mixing (FWM) and six-wave mixing (SWM) under EIT condition[1–3]. In the meantime, the fluorescence owing to spontaneous emission is also observed[4–6]. Moreover, the enhancement and suppression of FWM (SWM) and fluorescence corresponding to electromagnetically induced absorption (EIA) and EIT has aroused much interest[7,8]. The switch between bright state (EIA in the transmitted probe signal and enhancement in FWM and fluorescence signals) and dark state (EIT in the transmitted probe signal and suppression in FWM and fluorescence signals) can be realized by controlling phase difference between the two circularly polarized components of a single coherent field[9]. In addition, the switch can also be obtained by manipulating the dressing field power and the probe detuning[8,10–12].

In this paper, we experimentally demonstrate the phase-modulated switch between enhancement and suppression of SWM and fluorescence signals for the first time. First, the phase modulated switch between bright and dark states is realized under self-dressing condition. Second, we study the phase modulated switch under multi-dressing condition including the external-dressing. At last, we observe the dependence of the measured signals on relative phase.

Results

Our experiment is carried out in a ^{85}Rb vapor cell. The energy levels $5S_{1/2}(F = 3)$, $5S_{1/2}(F = 2)$, $5P_{3/2}$, $5D_{3/2}$, and $5D_{5/2}$ constitute a five-level atomic system(Fig. 1(a)). The transition $5S_{1/2}(F = 3)$ ($|0\rangle$) $- 5P_{3/2}$ ($|1\rangle$) is probed by the laser beam E_1 (frequency ω_1, wave vector $\mathbf{k}_1$ and Rabi frequency G_1). The transition $5P_{3/2} - 5S_{1/2}(F = 2)$ ($|3\rangle$) is driven by two coupling beams E_3 (ω_3, $\mathbf{k}_3$ and G_3) and E_3' (ω_3, $\mathbf{k}_3'$ and G_3'). Two dressing beams E_2 (ω_2, $\mathbf{k}_2$ and G_2) and E_4 (ω_4, $\mathbf{k}_4$ and G_4) respectively drive the upper transitions $5P_{3/2} - 5D_{5/2}$ ($|2\rangle$) and $5P_{3/2} - 5D_{3/2}$ ($|4\rangle$). In normal experiment, the five beams are placed in a square-box pattern (Fig. 1(b)). The beams E_2, E_4, E_3 and E_3' propagate through the cell in the same direction with tiny angles about $0.3°$ between any two. In the opposite direction of E_2 there is the probe beam E_1. However, in our experiment, the normal experimental configuration should be modified since we study the phase-controlled switch. The coupling beam E_2 (E_4) is deviated with an angle α (β) from the normal position (Fig. 1(c) and 1(d)). In the experimental system, we use E_{S1} and E_{S2} to represent the SWM signals generated by E_1, E_3, E_3' and E_2 and by E_1, E_3, E_3' and E_4, respectively. Besides, the single-photon fluorescence caused by the photon decay from the level $|1\rangle$ is called R_0. The sign R_1 (R_2) denotes the fluorescence due to the photon decay from the level $|2\rangle$ ($|4\rangle$).

Generally, we can obtain the density matrix elements $\rho_{10}^{(1)}$ (related with EIT), $\rho_{S1}^{(5)}$ (related with SWM signal), and $\rho_{11}^{(2)}, \rho_{11}'^{(2)}, \rho_{22}^{(4)}$ and $\rho_{33}^{(4)}$ (related with fluorescence R_0, R_1 and R_2) by solving the density-matrix equations. With Liouville pathway $\rho_{00}^{(0)} \xrightarrow{E_1} \rho_{10}^{(1)}$ and E_4 blocked, we can obtain
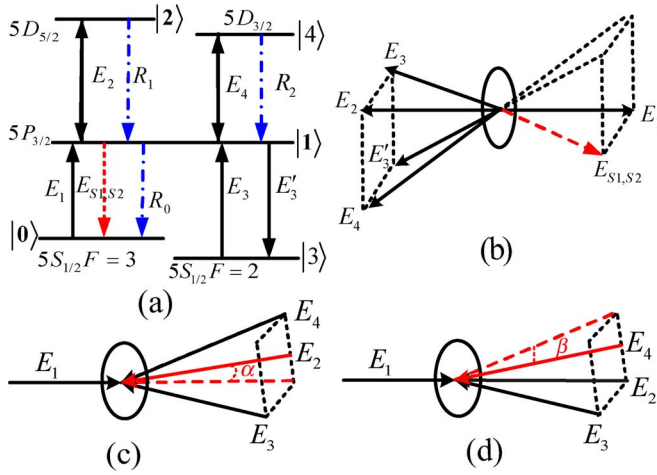
Figure 1 | (a) Relevant ^{85}Rb five-level atomic system.(b) Normal phase-matching configuration. (c) and (d) Abnormal configurations with the deflection angle α and β.

$$\rho_{10S}^{(1)} = iG_1/(d_1 + |G_2|^2 e^{i\Delta\Phi_1}/d_2) \qquad (1)$$

where $d_1 = i\Delta_1 + \Gamma_{10}$, $d_2 = i(\Delta_1 + \Delta_2) + \Gamma_{20}$, $\Delta_i = \Omega_i - \omega_i$ (Ω_i denotes the level resonance frequency and Γ_{ij} denotes the transverse relaxation rate between states $|i\rangle$ and $|j\rangle$). Significantly, the phase factor $e^{i\Delta\Phi_1}$ ($\Delta\Phi_1$ is related with the orientations of induced dipole moments μ_1 and μ_2[12]) has been introduced into the dressing term $|G_2|^2/d_2$ in $\rho_{10S}^{(1)}$ since the angle α between E_2 and the opposite direction of E_1 is considered. With all five beams including E_4 turned on, $\rho_{10S}^{(1)}$ is modified as

$$\rho_{10D}^{(1)} = iG_1/(d_1 + |G_2|^2 e^{i\Delta\Phi_1}/d_2 + |G_4|^2 e^{i\Delta\Phi_2}/d_4) \qquad (2)$$

with $d_4 = i(\Delta_1 + \Delta_4) + \Gamma_{40}$, where $\Delta\Phi_2$ is the phase factor related with the angle β. Via the Liouville pathway $\rho_{00}^{(0)} \xrightarrow{G_1} \rho_{10}^{(1)} \xrightarrow{(G_3')^*} \rho_{30}^{(2)} \xrightarrow{G_3} \rho_{10}^{(3)} \xrightarrow{G_2} \rho_{20}^{(4)} \xrightarrow{G_2^*} \rho_{10}^{(5)}$, the SWM signal E_{S1} can be obtained as

$$\rho_{S1}^{(5)} = G_A e^{i k_{S1}\cdot r}/[d_3(d_1 + |G_2|^2 e^{i\Delta\Phi_1}/d_2)^3(d_2 + |G_1|^2/d_5)] \qquad (3)$$

with E_4 blocked or

$$\rho_{D1}^{(5)} = G_A e^{i k_{S1}\cdot r}/$$
$$[d_3(d_1 + |G_1|^2/d_6 + |G_2|^2 e^{i\Delta\Phi_1}/d_2 + |G_4|^2 e^{i\Delta\Phi_2}/d_4)^3(d_2 + |G_1|^2/d_5)] \qquad (4)$$

with all five beams turned on, where $G_A = iG_1 G_3 G_3'^* G_2 G_2^*$, $d_3 = i(\Delta_1 - \Delta_3) + \Gamma_{30}$, $d_5 = \Gamma_{21} + i\Delta_2 + |G_3|^2/[\Gamma_{23} + i(\Delta_2 + \Delta_3)]$ and $d_6 = \Gamma_{11} + |G_4|^2 e^{i\Delta\Phi_2}/(\Gamma_{41} + i\Delta_4)$. Similarly, the SWM E_{S2} can be described by

$$\rho_{S2}^{(5)} = G_B e^{i k_{S2}\cdot r}/[d_3(d_1 + |G_4|^2 e^{i\Delta\Phi_2}/d_4)^3(d_4 + |G_1|^2/d_7)] \qquad (5)$$

with $G_B = iG_1 G_3 G_3'^* G_4 G_4^*$ and $d_7 = \Gamma_{41} + i\Delta_4 + |G_3|^2/[\Gamma_{43} + i(\Delta_4 + \Delta_3)]$ and

$$\rho_{D2}^{(5)} = G_B e^{i k_{S2}\cdot r}/$$
$$[d_3(d_1 + |G_1|^2/d_8 + |G_2|^2 e^{i\Delta\Phi_1}/d_2 + |G_4|^2 e^{i\Delta\Phi_2}/d_4)^3(d_4 + |G_1|^2/d_7)] \qquad (6)$$

with $d_8 = \Gamma_{11} + |G_2|^2 e^{i\Delta\Phi_1}/(\Gamma_{21} + i\Delta_2)$ under self-dressing (the self-dressing effect refer to that one of the participating fields for generating SWM signals dresses the involved energy levels, which then modifies the SWM process itself, for example, the term $|G_4|^2 e^{i\Delta\Phi_2}/d_4$

is the self-dressing term) and external dressing (the external-dressing effect refer to that the field will dresses the involved energy levels to modify the signals, while it is not the participated field for the generation of these signals, for example, the term $|G_2|^2 e^{i\Delta\Phi_1}/d_2$ is the external dressing term) condition, respectively. For the fluorescence signals, via the Liouville pathway $\rho_{00}^{(0)} \xrightarrow{E_1} \rho_{10}^{(1)} \xrightarrow{(E_1)^*} \rho_{11}^{(2)}$, one can obtain

$$\rho_{11S}^{(2)} = -|G_1|^2/[\Gamma_{11}(d_1 + |G_2|^2 e^{i\Delta\Phi_1}/d_2)] \qquad (7)$$

or

$$\rho_{11D}^{(2)} = -|G_1|^2/[\Gamma_{11}(d_1 + |G_2|^2 e^{i\Delta\Phi_1}/d_2 + |G_4|^2 e^{i\Delta\Phi_2}/d_4)] \qquad (8)$$

to describe the profile of fluorescence R_0 under single-dressing or double-dressing case, respectively. With the pathway $\rho_{33}^{(0)} \xrightarrow{E_3} \rho_{13}^{(1)} \xrightarrow{(E_3')^*} \rho_{11}^{(2)}$, one can acquire

$$\rho_{11}'^{(2)} = -|G_3|^2/[\Gamma_{11}(\Gamma_{13} + i\Delta_3)] \qquad (9)$$

to describe the DC background of R_0. Consequently, the fluorescence R_0 is proportional to $\left|\rho_{11D}^{(2)}\right|^2 + \left|\rho_{11}'^{(2)}\right|^2$. For two-photon fluorescence R_1, via $\rho_{00}^{(0)} \xrightarrow{E_1} \rho_{10}^{(1)} \xrightarrow{E_2} \rho_{20}^{(2)} \xrightarrow{(E_1)^*} \rho_{21}^{(3)} \xrightarrow{(E_2)^*} \rho_{22}^{(4)}$, we have

$$\rho_{22S}^{(4)} = |G_1|^2 |G_2|^2/[\Gamma_{22} d_1 d_9(d_2 + |G_2|^2 e^{i\Delta\Phi_1}/d_1)] \qquad (10)$$

with $d_9 = \Gamma_{21} + i\Delta_2$. Similarly, the other two-photon fluorescence R_2 is described as

$$\rho_{44S}^{(4)} = |G_1|^2 |G_4|^2/[\Gamma_{44} d_1 d_{10}(d_4 + |G_4|^2 e^{i\Delta\Phi_2}/d_1)] \qquad (11)$$

with $d_{10} = \Gamma_{41} + i\Delta_4$.

First, we consider the phase-modulated switch of self-dressed signals as shown in Fig. 2. In the experiment, we turn on E_1, E_2, E_3', E_3 and block E_4 and the signals are obtained by scanning Δ_2 at different discrete designated Δ_1 with $\Delta\Phi_1 = 0$ (Fig. 2(a), viewed as the reference point at the normal configuration), $\Delta\Phi_1 = -\pi/5$ (Fig. 2(b)) and $\Delta\Phi_1 = 3\pi/5$ (Fig. 2(c)). In Fig. 2(a1), the EIT caused by E_2, meeting $\Delta_1 + \Delta_2 = 0$, emerges in the larger range of the probe detuning. The EIA, satisfying $\Delta_1 + \Delta_2 = |G_2|^2/\Delta_1$, only appears at the large probe detuning, such as $\Delta_1 = \pm 400$ MHz. In Fig. 2(b1), we can find the probe transmission signals present as EIT at negative detunings Δ_1 while change from strong EIT to partial-EIT-partial-EIA and lastly to week EIA with Δ_1 increasing at positive detunings Δ_1. In Fig. 2(c1), with the probe detuning transformed from negative to positive, the signals turn from EIA to partial-EIT-partial-EIA and lastly to EIT. Obviously, the variations of the probe transmission signals are quite the contrary in above three figures. This is caused by the modulation of the relative phase $\Delta\Phi_1$ in the dressing term $|G_2|^2 e^{i\Delta\Phi_1}/d_2$ in $\rho_{10DD}^{(1)}$. Thus, at a certain detuning Δ_1, we can switch EIT and EIA by adjusting the relative phase $\Delta\Phi_1$. Similarly, the dressing effect on the SWM signal caused by $|G_2|^2 e^{i\Delta\Phi_1}/d_2$ is also regulated by $\Delta\Phi_1$. According to $\rho_{S1}^{(5)}$, the intensity of SWM has inverse correlation with $\cos(\Delta\Phi_1 - \theta)$ where $\theta = \arctan(\Delta_1/\Gamma_{10})$. In the SWM signals, with the relative phase $\Delta\Phi_1$ changed from 0 (Fig. 2(a2)) to $-\pi/5$ (Fig. 2(b2)), the intensity of SWM is obviously enhanced at $\Delta_1 \geq 0$ since $\cos(-\pi/5 - \theta) < \cos(0 - \theta)$ in the region while is suppressed at $\Delta_1 < 0$ for $\cos(-\pi/5 - \theta) > \cos(0 - \theta)$ here. One can also see the difference between the SWM signals with $\Delta\Phi_1 = 0$ (Fig. 2(a2)) and those with $\Delta\Phi_1 = 3\pi/5$ (Fig. 2(c2)). Compared with the SWM in Fig. 2(a2), the SWM signal in Fig. 2(c2) is suppressed in
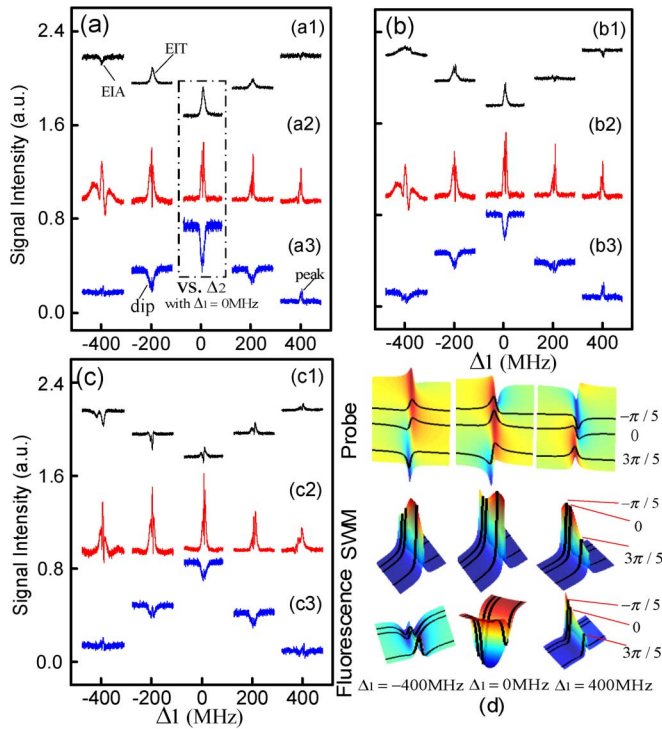
Figure 2 | In each sub-curve, measured probe transmission signals ((a1), (b1) and (c1)), SWM signals ((a2), (b2) and (c2)) and fluorescence signals ((a3), (b3) and (c3)) versus Δ_2 (Δ_2 is scanned around $-\Delta_1$ from -90 MHz to 90 MHz) with E_4 blocked. Each sub-curve corresponds to different fixed Δ_1. For (a1)–(a3) $\Delta\Phi_1 = 0$, for (b1)–(b3) $\Delta\Phi_1 = -\pi/5$ and for (c1)–(c3) $\Delta\Phi_1 = 3\pi/5$. The other parameters are $\Delta_3 = 0$, $G_1 = 10.85$ MHz, $G_2 = 19.46$ MHz, $G_3 = 16.66$ MHz and $G_3' = 14.4$ MHz. (d) Theoretical calculations for probe, SWM and fluorescence signals versus $\Delta\Phi_1$ by scanning Δ_2 at three typical detunings Δ_1.

the region $\Delta_1 \gtrsim 200$ MHz and enhanced in the region $\Delta_1 < 200$ MHz. From Fig. 2(a3) to Fig. 2(b3), one can find, with EIT converted to EIA (for example, at $\Delta_1 = 200$ MHz from Fig. 2(a1) to Fig. 2(b1)), on one hand, the dip of the corresponding fluorescence gets shallow due to the weakened dressing effect of E_2 on R_0 (in company with EIA) according to $\rho_{11S}^{(2)}$, on the other hand, the peaks in the dips get high because the original suppression (in company with EIT) induced by the dressing term $|G_2|^2 e^{i\Delta\Phi_1}/d_2$ in $\rho_{22S}^{(4)}$ turns to enhancement (in company with EIA). While EIA (Fig. 2(a1)) is converted to EIT (Fig. 2(b1)), for example, at $\Delta_1 = -400$ MHz, the variations of the fluorescence signals are just the opposite. Same as above, when $\Delta\Phi_1$ is changed from 0 (Fig. 2(a3)) to $3\pi/5$ (Fig. 2(c3)), the similar variations also appear in the fluorescence signals, for example, at $\Delta_1 = -200$ MHz and $\Delta_1 = 400$ MHz. We have simulated the EIA-EIT switch in the probe transmission signal and suppression-enhancement transformation in SWM and fluorescence process, as shown in Fig. 2(d) which agrees with the experimental results very well.

Further, we turn on all five laser beams including E_4 and observe the phase controlled switch of the multi-dressed (the multi-dressing effect is the case where two or more fields including self- and external-dressing fields dress the energy levels to modify the signals) signals by scanning Δ_4 at different discrete fixed Δ_1 (Fig. 3). In Fig. 3(a1), the peak higher than the baseline in each sub-curve represents the EIT induced by E_4. The global profile formed from all baselines means the EIT induced by E_2, meeting the condition $\Delta_1 + \Delta_2 = 0$. When we change the related phase $\Delta\Phi_2$ from 0 (Fig. 3(a1)) to $\pi/2$ (Fig. 3(a2)), the original EITs are mostly switched to EIA. In Fig. 3(b1), the dip in each sub-curve shows the suppression on R_0
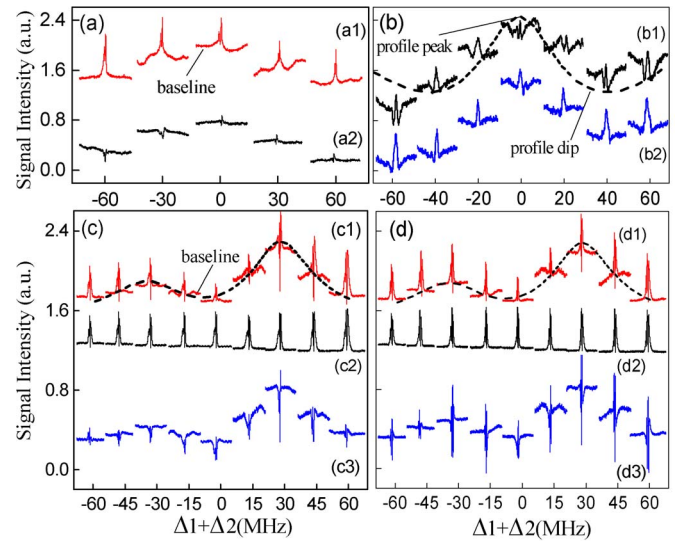

Figure 3 | In each sub-curve, measured probe transmission signals (a), fluorescence signals (b), and SWM signals (c)–(d) versus Δ_4 (Δ_4 is scanned around $-\Delta_1$ from -90 MHz to 90 MHz) with the fixed Δ_2. Each sub-curve corresponds to different discrete fixed Δ_1. (a1), (b1) and (c) Signals obtained with $\Delta\Phi_2 = 0$. (a2), (b2) and (d) Signals obtained with $\Delta\Phi_2 = \pi/2$. (a), (b), (c1) and (d1) Signals obtained with all beams turned on. (c2) and (d2) Signals obtained with E_2 blocked. (c3) Signals obtained by subtracting the signals in (c2) from the signals in (c1). (d3) Signals obtained by subtracting the signals in (d2) from the signals in (d1). Other parameters are $\Delta_2 = 100$ MHz, $\Delta_3 = 0$, $\Delta\Phi_1 = 0$, $G_1 = 10.72$ MHz, $G_2 = 21.16$ MHz, $G_3 = 18.87$ MHz, $G_3' = 14.4$ MHz and $G_4 = 14.16$ MHz.

caused by the dressing field E_4 and the peak in each dip represents the two-photon fluorescence R_2. The profile dip consisting of baselines reveals R_0 suppressed by E_2 owing to the dressing term $|G_2|^2/d_2$ in $\rho_{11D}^{(2)}$ and the profile peak represents the two-photon fluorescence R_1. With $\Delta\Phi_2$ changed from 0 (Fig. 3(b1)) to $\pi/2$ (Fig. 3(b2)), the height of the peak in each sub-curve gets much high because the dressing term $|G_4|^2 e^{i\Delta\Phi_2}/d_1$ in $\rho_{44S}^{(4)}$ has generated the enhancement effect on R_2 at $\Delta\Phi_2 = \pi/2$. In this process, the dip in each sub-curve becomes shallow due to the weakened dressing effect of E_4 on R_0 caused by the modulation of $\Delta\Phi_2$.

In Fig. 3(c1), the global profile (dashed curve) consisting of all baselines reveals the SWM signal E_{S1}. In the E_{S1} signal, one can find the AT splitting which is because the self-dressing term $|G_1|^2/d_5$ acts on the two-photon term d_2 in $\rho_{D1}^{(5)}$. The sub-curve at any Δ_1 means the compound signal which includes two components: I_{D1} and I_{D2}. I_{D1} denotes the enhancement or suppression intensity of E_{S1} (arising from the external-dressing field E_4 according to $\rho_{D1}^{(5)}$) and I_{D2} signifies the SWM E_{S2} intensity with the suppression of E_2. Figure 3(c2) shows the SWM E_{S2} intensity without the suppression of E_2 which is denoted by I_{S2}. The signals in Fig. 3(c3) are obtained by subtracting the signals (I_{S2}) in Fig. 3(c2) from the signals ($I_{D1} + I_{D2}$) in Fig. 3(c1). Therefore, the signals in Fig. 3(c3) represent two dressing results at different Δ_1: one is I_{D1}, the other is I_{D2}-I_{S2} which is the suppressed intensity caused by E_2 with regard to the SWM E_{S2}. When we alter the relative phase $\Delta\Phi_2$, the experiment results similar to Fig. 3(c) are obtained, as shown in Fig. 3(d1)–3(d3). The modulation of signals caused by relative phase can be observed clearly, as shown in Fig. 3(c3) and Fig. 3(d3). For instance, with the relative phase switched from 0 to $\pi/2$, the original suppression signals (at $\Delta_1 + \Delta_2 = -45, -30$ and -15 MHz) transform into partial-suppression-partial-enhancement signals and the intensities of original partial-suppression-partial-enhancement signals (at $\Delta_1 + \Delta_2 = 0, 15, 30, 45$ and 60 MHz) are strengthened significantly in correspondence with

the EIT-EIA switch in Fig. 3(a). It is worth mentioning that the dressing result of E_2 is basically invariable since the relative phase $\Delta\Phi_2$ is only related to the dressing effect of E_4.

Discussion

In order to clearly compare the variations of signals with the relative phase, we discuss the relative phase dependence of the measured signals by scanning Δ_4 at the fixed detuning Δ_1 under the above mentioned two cases of self-dressing and multi-dressing effects. First, with E_2 blocked (Fig. 4(a), the self-dressing case), EIT in Fig. 4(a1) can be switched to EIA along with the change of $\Delta\Phi_2$ from bottom to top. During this process, the strongest EIT and EIA separately appear at $\Delta\Phi_2 = -\pi/6$ and $\Delta\Phi_2 = 3\pi/4$. Depending on whether $\Delta\Phi_2$ is greater than or less than $\pi/4$, the transmitted probe signal behaves mainly EIA or EIT. In the phase matching range where $\Delta\Phi_2$ is altered from $-\pi/6$ to $\pi/2$, compared with the signals at the reference phase $\Delta\Phi_2 = 0$, the SWM signal E_{S2} (Fig. 4(a2)) and fluorescence signal R_2 (peaks in Fig. 4(a3)) get large when $\Delta\Phi_2 > 0$ and become small while $\Delta\Phi_2 < 0$ due to the switch of the dressing effect of E_4 induced by $\Delta\Phi_2$. The largest intensities of the SWM and fluorescence signals appear at partial-EIT-partial-EIA ($\Delta\Phi_2 = \pi/4$) and EIA ($\Delta\Phi_2 = \pi/2$), respectively. Along with continuing to increase $\Delta\Phi_2$ from $\pi/2$ to π or to decrease $\Delta\Phi_2$ from $-\pi/6$ to $-\pi/3$, which correspond to increasing the deflection angle β under the abnormal configuration (Fig. 1(d)), the SWM and fluorescence signal intensities decrease. This results from the classical effect with the

phase mismatching condition. For the sake of clarity, the relative phase dependence of the fluorescence peak R_2 is also shown by dash line with circles in Fig. 4(a4). The fluorescence suppression dip (Fig. 4(a3)) induced by E_4 evolves from shallow to deep, then to shallow, the variation of which with the relative phase is also illustrated by the solid line with squares in Fig. 4(a4). The fluorescence suppression dip reaches the deepest at the stronger EIT. Next, with all five beams on (Fig. 4(b), the multi-dressing case), the evolvement of probe transmission signal in Fig. 4(b1) is similar to that in Fig. 4(a1) except that the EIT peak in Fig. 4(b1) is weaker than the one in Fig. 4(a1) due to the strong cascade-dressing interaction between E_2 and E_4. The peaks higher than the baselines in Fig. 4(b2) show the variation of the intensity I_{D2} of SWM signal E_{S2} under the dressing effect of E_2, the evolvement of which approximates to that of the SWM peaks in Fig. 4(a2). The dips lower than the baselines in Fig. 4(b2) illustrate the variation of the suppression signal intensity I_{D1} of SWM E_{S1}. In the phase matching range, the suppression dips of SWM E_{S1} are relatively deep under the condition of EIT and become shallow in the case of EIA. The variations of fluorescence peak R_2 and fluorescence suppression dip in Fig. 4(b3), the relative phase dependences of which are shown in Fig. 4(b4), accord with those in Fig. 4(a3) except that the peaks become slightly small and the dips get shallow because of the cascade-dressing interaction between E_2 and E_4.

In summary, we study the phase modulated switch between suppression and enhancement of fluorescence and SWM. By manipulating the relative phase, the original suppression on SWM and fluorescence signals can be transformed into enhancement in company with the conversion from EIT to EIA in the transmitted probe. Such switch can be applied in optical communication and quantum information processing.

Methods

In our experiment, there are five laser beams generated by four external cavity diode lasers (ECDL) with linewidths of less than or equal to 1 MHz. The probe laser beam E_1 is from an ECDL with wavelength of 780.245 nm and a horizontal polarization. The two coupling laser beams E_3 and E_3' with wavelength 780.235 nm and a vertical polarization are split from another ECDL. The dressing laser beam E_2 (E_4) with wavelength of 775.978 nm (776.157 nm) and a vertical polarization are from other two ECDLs. The atomic vapor cell temperature is set at 60°C, corresponding to the typical density of 2×10^{11} cm^{-3}. In our five-level atomic system, there exist two ladder-type EIT windows, two SWM signals and three fluorescence signals under the normal experimental configuration (Fig. 1(b)). Specifically, one SWM signal E_{S1} is generated by E_1, E_3, E_3', and E_2 in the $|0\rangle - |1\rangle - |2\rangle$ ladder-type EIT window, which satisfies the phase matching condition $\mathbf{k}_{S1} = \mathbf{k}_1 + \mathbf{k}_3 - \mathbf{k}_3' + \mathbf{k}_2 - \mathbf{k}_2$, and the other SWM signal E_{S1} is generated by E_1, E_3, E_3' and E_4 in the $|0\rangle - |1\rangle - |4\rangle$ ladder-type EIT window, which satisfies the phase matching condition $\mathbf{k}_{S2} = \mathbf{k}_1 + \mathbf{k}_3 - \mathbf{k}_3' + \mathbf{k}_4 - \mathbf{k}_4$. Besides, the single-photon fluorescence R_0 is caused by the photon decay from the level $|1\rangle$. The two-photon fluorescence R_1 and R_2 are due to the photon decay from the level $|2\rangle$ and $|4\rangle$, respectively. When the coupling beam E_2 (E_4) is deviated with an angle α (β) from the normal position (Fig. 1(c) and 1(d)), the above EIT windows, SWM and fluorescence signals will switch between bright state (EIA in the transmitted probe signal and enhancement in SWM and fluorescence signals) and dark state (EIT in the transmitted probe signal and suppression in SWM and fluorescence signals).
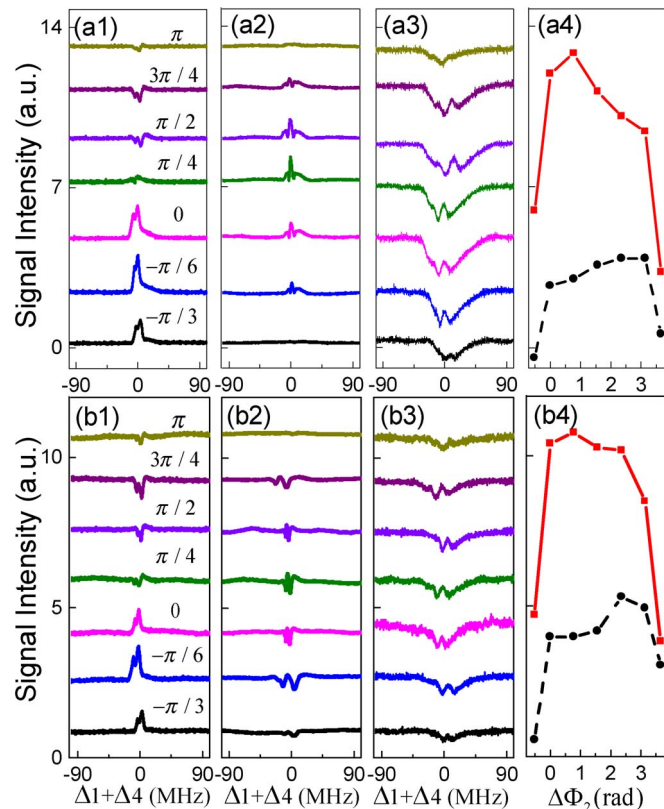

Figure 4 | The transmitted probe ((a1), (b1)), SWM ((a2), (b2)) and fluorescence ((a3), (b3)) versus Δ_4 at different relative phase $\Delta\Phi_2 = -\pi/3$, $-\pi/6$, 0, $\pi/4$, $\pi/2$, $3\pi/4$, and π from the bottom to top.(a1),(a2) and (a3) Signals obtained with E_2 blocked. (b1),(b2) and (b3) Signals obtained with all beams turned on. (a4) and (b4) the relative phase dependences of the fluorescence peak (dash line with circles) and the fluorescence dip (solid line with squares) in (a3) and (b3), respectively. The other parameters are $\Delta\Phi_1 = 0$, $\Delta_1 = -120$ MHz, $\Delta_2 = 150$ MHz, $\Delta_3 = 0$, $G_1 = 11.84$ MHz, $G_3 = 18.34$ MHz, $G_3' = 17$ MHz, $G_2 = 26.11$ MHz and $G_4 = 18$ MHz.

1. Wielandy, S. & Gaeta, A. Investigation of electromagnetically induced transparency in the strong probe regime. *Phys. Rev. A* **58**, 2500–2505 (1998).
2. Kash, M. *et al.* Ultraslow group velocity and enhanced nonlinear optical effects in a coherently driven hot atomic gas. *Phys. Rev. Lett.* **82**, 5229–5232 (1999).
3. Ham, B. S., Shahriar, M. S. & Hemmer, P. R. Enhanced nondegenerate four-wave mixing owing to electromagnetically induced transparency in a spectral hole-burning crystal. *Opt. Lett.* **22**, 1138–1140 (1997).
4. Harris, S. E. Electromagnetically induced transparency. *Phys, Today* **50**, 36–42 (1997).
5. Qi, J. *et al.* Autler-Townes splitting in molecular lithium: Prospects for all-optical alignment of nonpolar molecules. *Phys. Rev. Lett.* **83**, 288–291 (1999).
6. Qi, J. & Lyyra, A. M. Electromagnetically induced transparency and dark fluorescence in a cascade three-level diatomic lithium system. *Phys. Rev. A*, **73**, 043810 (2006).
7. Akulshin, A. M., Barreiro, S. & Lezama, A. Electromagnetically induced absorption and transparency due to resonant two-field excitation of quasidegenerate levels in Rb vapor. *Phys. Rev. A* **57**, 2996–3002 (1998).

8. Li, N. *et al.* Observation of dressed odd-order multi-wave mixing in five-level atomic medium. *Opt. Exp.* **20**, 1912–1929 (2012).
9. Khadka, U., Zhang, Y. P. & Xiao, M. Control of multitransparency windows via dark-state phase manipulation. *Phys. Rev. A*, **81**, 023830 (2010).
10. Li, C. *et al.* Observation of enhancement and suppression in four-wave mixing processes. *Appl. Phys. Lett.* **95**, 041103 (2009).
11. Wang, Z. *et al.* Switching enhancement and suppression of four-wave mixing via a dressing field. *J. Mod. Opt.* **58**, 802–809 (2011).
12. Hahn, K. H., King, D. A. & Harris, S. E. Nonlinear generation of 104.8-nm radiation within an absorption window in zinc. *Phys. Rev. Lett.* **65**, 2777–2779 (1990).

Acknowledgments

Author contributions

Z.G.W. and Y.P.Z. provided the idea and main contributions to the theoretical and experimental analysis of this work. P.Y., P.Y.L., D.Z., H.Q.H. and H.T. contributed to the presentation and execution of the work. All authors discussed the results and contributed to writing the manuscript.

Additional information